PHYSICAL REVIEW B VOLUME 2, NUMBER 2 15 JULY 1970

Optical Properties of Amorphous Germanium Films*

T. M. Donovan† and W. E. Spicer

Stanford University, Stanford, California 94305

and

J. M. Bennett and E. J. Ashley

Michelson Laboratory, China Lake, California 93555

(Received 5 January 1970)

The optical constants of amorphous Ge films formed under well-defined conditions have been determined in the 0.1–25.0-eV spectral range. In the 0.1–1.8-eV range they were determined by analysis of precise reflectance and transmittance data (RT), and in the 0.1–25.0-eV range by a Kramers-Kronig analysis of normal-incidence reflectance data. Both analyses gave the same results in the region of overlap. The absorption edge was found to be quite sharp (0.06 eV) and to occur usually at a photon energy of about 0.6 eV. The position of the edge was normally about 0.2 eV lower than the direct edge in crystalline Ge. No evidence was found for either the spin-orbit split valence band associated with crystalline Ge or a tailing and/or large number of states in the forbidden region. The smallest nonzero value of the absorption measured on the low-energy side of the absorption edge was about 10 cm^{-1}. There was no evidence for free-carrier absorption further in the infrared. At 0.1 eV, the index of refraction was 3.99 ± 0.04 as determined by the RT analysis. This value was in excellent agreement with the value of 4.00 derived from the zero-frequency dielectric constant, which has been calculated using the sum rule. This is also the value determined for crystalline Ge in the infrared. Reflectance data for amorphous Ge films deposited and measured in ultra-high vacuum (*in situ*) are reported for the region 2.0–11.8 eV. The density, determined by weighing films of known thickness, was 12–15% less than the density of crystalline Ge.

I. INTRODUCTION

Changes in photoemission and optical properties related to the loss of long-range order have been observed in studies of crystalline and amorphous germanium.[1–3] Photoemission studies[3] have indicated that the density of states of the amorphous phase differs from that of crystalline Ge in two important respects: The sharp structure in the density of states which characterizes crystalline Ge is completely missing, and the valence band appears to have narrowed with a marked increase in the number of states appearing within 1 eV of the band maximum.

Herman and Van Dyke[4] have shown that this latter effect would be expected if a density for the amorphous phase 28% less than the crystalline density was used in the band calculation. Their calculation, however, does not take the disordered nature of these films into account, and the average lattice dilation used in the calculation was based on a larger density change than is now thought to exist. Other authors,[5–7] taking disorder into account in calculating the electronic structure of amorphous solids, have discussed the possibility of the loss of a sharply defined band edge and a "tailing" of large numbers of localized states in the forbidden region. The exponential absorption in the region of the absorption edge observed by Clark[8] might be interpreted as a tailing of states into the forbidden region; however, Clark did not measure values of α less than 500 cm^{-1}. Other optical studies of amorphous Ge[2,9] have shown the lack of a well-defined band edge, in qualitative support of theoretical expectations, and a recent spin-resonance study[10] has measured 10^{20} states/cm^3 in amorphous Ge which have been associated with surface states found in crystalline Ge.

In the photoemission studies[3] we found evidence neither for band tailing nor for extremely large numbers of states in the forbidden region. The widths of the energy distribution curves (EDC's) for amorphous Ge were approximately the same, and the leading edges were nearly as sharp as the crystalline EDC's. To determine the form of the empty state density in the region below the vacuum level, which is inaccessible to photoemission, and to estimate the density of states in the forbidden region, it was decided to measure the optical properties of amorphous Ge films in the absorption-edge region, using films that had been prepared under vacuum conditions comparable to those used in the photoemission studies. Preliminary precision optical experiments[11] showed that amorphous

Ge had a sharp absorption edge at an energy somewhat lower than that of crystalline Ge. No absorption was found further in the infrared which could be associated with free-carrier absorption. The recent work of Tauc *et al.*[9a] is in agreement with the latter result and in disagreement with Tauc's earlier findings.[2]

In the previously reported work,[11] an optical density of states consistent with both the photoemission and optical data was derived using the nondirect constant matrix element model. More recently, Brust[12a] used a band model in the first approximation with direct transitions, disorder scattering, and a density dilation to directly calculate the optical properties and photoemission results. This approach appears to predict, qualitatively, the sharp and shifted absorption edge observed in this study.

In this paper we present a detailed description of the studies of the optical properties of amorphous Ge films; this work was presented in a preliminary form in the paper referred to above.[11] All the films discussed in this paper showed no evidence of crystallinity, i.e., they showed the diffuse electron diffraction patterns which generally characterize amorphous Ge. The optical constants have been determined in the region of the absorption edge and at lower energies (0.1–1.8 eV) using precision normal-incidence reflectance and transmittance measurements. In the transparent region below the absorption edge the absorption is very small. In order to measure it accurately, we have used films up to 2 μ thick, which were extremely uniform in thickness. We were not able to produce films thicker than 2 μ that were uniform in thickness and free from defects such as cracks and pinholes. Chopra and Bahl[12b] have apparently been able to produce films up to 10 μ in thickness which are free of macroscopic defects. These authors point out, however, that for films thicker than about 7 μ (using their evaporation conditions), partial crystallization of the films can occur, possibly due to heating by radiation from the source or due to the heat of condensation of the vapor beam. For films up to 7 μ thick, these authors have observed a sharp absorption edge, in qualitative agreement with our results.

We have also determined the optical constants of films in the 0.1–25.0-eV range by a Kramers-Kronig (KK) analysis of the normal-incidence reflectance. In the preliminary study[11] we used the optical data of Marton and Toots (MT)[13] in the range 8.0–25.0 eV. Here we report new measurements for a film prepared and measured in ultrahigh vacuum in the 2.0–11.8-eV range; these results are used in a new KK analysis. Sum-rule calculations using the optical constants derived from the KK analysis have yielded values of the static dielectric constant and the effective number of electrons per atom involved in the transitions occurring within the range of these measurements. The density of Ge derived from the sum-rule calculations is compared with the density determined by weighing films similar to those used for the optical measurements.

II. EXPERIMENTAL

Infrared and Visible Reflectance and Transmittance Measurements

Amorphous Ge films were prepared by evaporation of intrinsic crystalline Ge in two different vacuum systems, one an oil-pumped system having a base pressure of 1×10^{-7} Torr and the other an ion-pumped baked ultrahigh vacuum system having a base pressure of $<1\times10^{-9}$ Torr. Pressures during evaporation were in the 5×10^{-7}–5×10^{-6}-Torr range for the standard vacuum system and in the 2×10^{-8}–5×10^{-8}-Torr range for the ultrahigh vacuum system. Evaporation sources were tungsten boats, Al_2O_3-coated molybdenum boats, and an electron beam gun; deposition rates were 10-50 Å/sec. In order to ensure that the films prepared in the standard vacuum system were uniform in thickness, a 20-in. source-to-substrate distance was used, and the four 1.520-in.-diam substrates were mounted on a turntable which rotated as a unit. In addition, each substrate turned on its own axis. In the ultrahigh vacuum system the source-to-substrate distance was 23 in., and the mean free path was long enough so that uniform films were produced without spinning the substrates. Substrates used in the experiments were fused-quartz optical flats with supersmooth surfaces (7 Å rms),[14] $\frac{1}{16}$-in.-thick commercially polished fused-silica windows (25 Å rms), and commercially polished KCl infrared windows (100 Å rms).

After an evaporation was completed, dry argon was let into the system to bring it up to atmospheric pressure, and the reflectance (R) and transmittance (T) measurements were made as soon as possible in a dry nitrogen atmosphere. The reflectometer has been described previously by Bennett and Koehler[15]; it measures the square of the absolute reflectance. Most of the major sources of systematic error have been either reduced or eliminated in the instrument. For example, the effect of sample tilt, a major source of error in reflectance measurements, has been eliminated by the double-reflection optical system. The accuracy of the measurements depends on the linearity of the entire detection system, i.e., whether the detector output is strictly proportional to the light flux falling on it. A three-polarizer method[16] was used to determine the linearity of the system,

which was found to be within ±0.001 over the entire range of intensities used. The reflectance measurements reported in this paper are believed to be good to ±0.001 and the transmittance measurements to ±0.002. Effects of substrate uniformity, scattering, matching of sample, and reference substrates, etc., limit the over-all accuracy of the transmittance measurements.

The thicknesses of the Ge films were measured interferrometrically using multiple beam fringes of equal chromatic order.[17] Each sample for thickness measurement was prepared at the same time as an R and T measurement sample and consisted of a supersmooth optical flat on which was evaporated a sharp-edged Ge strip down the center. The sample was overcoated with an opaque layer of silver, and the Ge film thickness was measured using the technique described in Ref. 17. The wavelengths of the fringes were determined visually by setting a crosshair on each fringe in turn and reading the wavelength on a direct-reading constant-deviation spectrometer. The setting accuracy was ~1 Å, making the thickness measurements good to ~±4 Å. In order to determine the uniformity of the films, the thickness was measured at various places on the sample. Film uniformity varied from ±4 Å on an 816-Å film to ±28 Å on a 20 654-Å film. As a further test of uniformity, the samples could be rotated in the R or T holders in the reflectometer without varying the measured R or T values by more than the measuring precision.

In order to show that the Ge films were really amorphous, they were studied using reflection electron diffraction. Thinner films on KCl (~1000 Å) were also studied using transmission electron diffraction and electron microscopy. All films were found to be amorphous. This result is to be expected since the substrate temperature during an evaporation remained within 1° of room temperature; it was well below the amorphous-crystalline transition temperature of 200–300° C for evaporated Ge.[18]

Visible and Ultraviolet Reflectance Measurements in Vacuum

For the *in situ* reflectance measurement in ultrahigh vacuum, intrinsic Ge was evaporated from a tungsten filament onto a float-glass substrate having a rms roughness of less than 20 Å and located 5 in. from the source. During evaporation, the pressure in the system (which had been baked out and was connected to a National Research Corporation Orb-Ion pump) rose to no more than 2×10^{-7} Torr and immediately fell back to the base pressure of 1×10^{-10} Torr after evaporation was completed.

The near-normal-incidence reflectance measurement was made in the same system immediately following evaporation, using the reflectometer developed by Endriz.[19] This reflectometer had a detection system consisting of a light pipe, sodium salicylate phosphor, and photomultiplier. The reflectance was measured at 0.2-eV intervals in the 2.0–11.8-eV region starting at the high-energy end, and all measurements were completed within a period of 4 h. During this time, the pressure was maintained at the base pressure of the system (1×10^{-10} Torr). The reflectance was periodically remeasured at several points such as 11.8 and 10.2 eV to check for contamination effects and, after 24 h, the entire set of reflectance measurements was repeated. No contamination effects were observed. The reflectance measurements were repeated again after the system had been let up to atmospheric pressure for 1 h and then reevacuated. A reflectance decrease, the exact amount of which depended on wavelength, was observed, which was presumably caused by the surface oxide layer.

The reflectance of this sample was also measured on the Bennett reflectometer in the 2.0–5.0-eV range; the agreement between the two instruments was better than ±0.005. This good agreement verifies the accuracy of the measurements made with the Endriz reflectometer. Since it uses a sodium salicylate phosphor in its detection system, any problems associated with the transparency of the sodium salicylate would occur in the above-measured region. Also, since the reflectometer gave correct results for the low-energy measurements, it should also give correct results at high energies, since probable sources of systematic error such as the alignment of the light pipe are independent of wavelength.

Film thickness was approximately determined using a crystal monitor during evaporation and was checked using the interferrometric technique mentioned above. The film was also observed by reflection electron diffraction and was found to be amorphous.

III. CALCULATION METHOD FOR DETERMINING OPTICAL CONSTANTS FROM R AND T MEASUREMENTS

The following procedure was used to obtain the optical constants of amorphous Ge in the infrared and absorption-edge regions from the measured reflectance, transmittance, and film thickness. The transmittance of the Ge-coated substrate was measured relative to that of an identical uncoated substrate, as indicated schematically in Fig. 1. In order to obtain the quantity T_f used in the multilayer film program,[20] the effect of the back surface of the substrate and multiple reflections in the

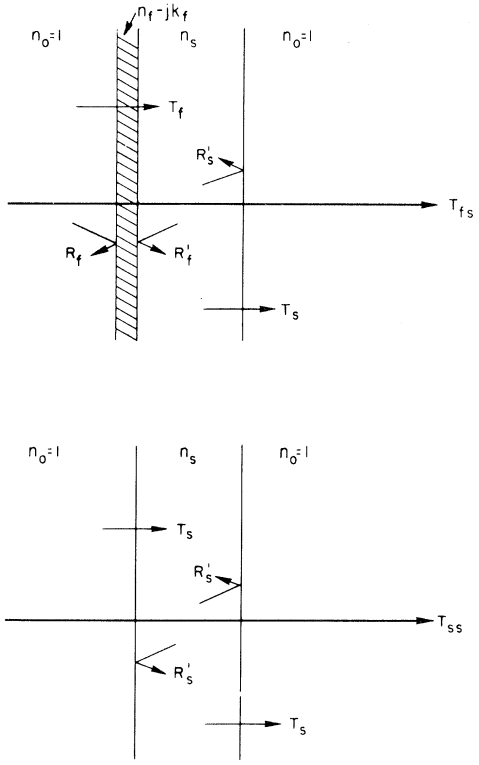

FIG. 1. Arrangement for obtaining the transmittance T_f and reflectance R_f of a Ge film (subscript f refers to the film and s to the uncoated substrate). The two substrates are matched for transmittance before the film is applied, and the transmittance ratio $T_{obs} = T_{fs}/T_{ss}$ is measured. The measured reflectance R_{obs} on the film-coated substrate includes the effect of reflection from the back surface of the substrate and multiple reflections within the substrate. Equations for obtaining T_f and R_f from the measured quantities are given in the text.

substrate had to be eliminated. This was accomplished using Eqs. (15) and (16) in Ref. 21:

$$T_f = T_{obs}(1 - R_f'R_s')/(1 + R_s') \quad , \tag{1}$$

where T_{obs} is the measured transmittance ratio T_{fs}/T_{ss}; $R_s' = (n_s - 1)^2/(n_s + 1)^2$, where n_s is the refractive index of the substrate; and R_f' is the reflectance at the substrate-film interface (see Fig. 1). Although R_f' is not known and must be calculated from the optical constants of the film and substrate, it is sufficiently close to the measured reflectance R_{obs} in this particular case that the latter quantity may be used in the calculations. This is the procedure we followed in this paper.

The reflectance R_{obs} was measured on the film-coated substrate when it was followed by a spacer and piece of black velvet. In this configuration, the back surface contributed to the reflectance and its effect was eliminated using Eq. (51) in Ref. 22. The expression for R_f is

$$R_f = R_{obs} - T_f^2 R_s'/(1 - R_f'R_s') \quad . \tag{2}$$

Equations (1) and (2) were derived assuming that multiple reflections occur in the substrate but that the multiply reflected beams are not coherent. Thus, the intensities of the beams rather than their amplitudes are summed. Although the substrates are considered nonabsorbing, a small amount of absorption or scattering is tolerable since the transmittance, which is most sensitive to attenuation of the beam in the substrate, is measured relative to that of an identical uncoated substrate and the attenuation occurs equally in both substrates.

After the quantities T_f and R_f were determined and the thickness of the Ge film was measured, the optical constants of Ge could be calculated using an iterative technique[23] which was a modification of our multilayer film program.[20] The basic program calculates R_f and T_f given the refractive index and thickness of the film and the refractive index of the substrate. The equations used in the program are in matrix form and are equivalent to the equations given by Hass for an absorbing film on an absorbing or nonabsorbing substrate.[24] In the iterative method used to obtain the optical constants $n - ik$ for Ge, several trial values of n were input, and the value was chosen which made the quantity $R_f - R_{calc}$ a minimum. (Here R_f is the input value and R_{calc} is the corresponding calculated quantity.) Similarly, a series of k values were input and the k value was saved, which minimized the quantity $T_f - T_{calc}$. The iterations were continued; each time the range of trial values of n and k was reduced until the differences $R_f - R_{calc}$ and $T_f - T_{calc}$ were within experimental measuring error.

IV. OPTICAL CONSTANTS IN THE INFRARED

Figures 2 and 3 show the reflectance and transmittance, respectively, in the wavelength range 1.0–4.0 μ (1.2–0.31 eV) for a 2138-Å-thick amorphous Ge film deposited on fused quartz. These data are used for an illustration of the analysis described above. The open circles are values of R_f and T_f derived from measured quantities, and the solid lines are drawn through values of R_{calc} and T_{calc} obtained from the multilayer film program using the optical constants of Ge calculated for this particular film. Measured, corrected, and calculated values of the reflectance and transmittance are listed in Table I along with values of n and k calculated for this film. Since the n and k values are smooth and the calculated and measured reflectances (and transmittances) agree, the data appear to be good to about the stated lim-

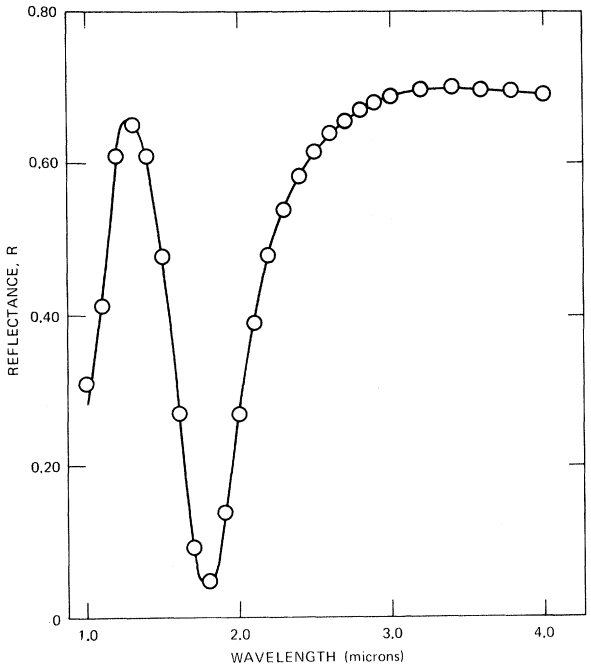

FIG. 2. Measured and calculated reflectance of a 2138-Å-thick Ge film. The open circles are values of R_f derived from the measured quantities and the solid line is drawn through values of R_{calc} obtained from the multilayer film program using optical constants for this particular film. Values of the reflectance, transmittance, and optical constants for this film are given in Table I.

its of accuracy.

The sum of R_f and T_f at wavelengths longer than 2.0 μ (0.6 eV) is approximately 1.00, indicating that the films are nonabsorbing in this region; i.e., k is very small. The average value of the sum in the 2.0–4.0-μ wavelength region is 1.004 ± 0.002, only slightly larger than the quoted error in the measurements. For an 816-Å-thick film this average sum was 1.001 ± 0.002, and for a 5371-Å film the sum was 1.003 ± 0.004. Several factors could be influencing the sums to make them larger than 1.000 ± 0.003. The uncoated and film-covered substrates could have slightly different absorptions, particularly at the longest wavelengths where the absorption in quartz becomes appreciable. (If *both* substrates have equal amounts of absorption, a simple calculation shows that the results will not be appreciably influenced by the absorption.) The average thickness of the Ge film could be slightly different for the reflectance measurements and for the transmittance measurements. Even though both measurements were made on the same sample to minimize this effect, different areas were illuminated, so that slight thickness variations in the film could influence the average thickness over a given area.

It was observed that the films did change with time. Absorption sometimes increased, as evidenced by changes in the magnitudes and wavelengths of the fringe maxima and minima, and pinholes appeared. Films thicker than those used in the measurements tended to crack and peel off the substrates. To minimize effects of aging, measurements were always made as soon as possible after the evaporations were completed, the reflectance being measured first and the transmittance second.

Average values of the refractive index n and the extinction coefficient k are plotted as circles in Figs. 4 and 5 for the energy range 0.2–1.8 eV. These were determined from a series of five films ranging in thickness from 816 to 5371 Å. The triangles are values obtained from a KK analysis and will be described in the next section. Smooth average curves are drawn through all the data points. Values of the optical constants for the individual films as well as the average values, are listed in Table II for the energy range 1.24–0.31 eV. With the exception of one film, which was deposited on a KCl substrate, all data in this region are for Ge films deposited on fused-quartz substrates.

In the 0.3–0.4-eV range, the average value of n for four films is 4.00 ± 0.01. The extinction coefficient k approaches zero at 0.58 eV and remains

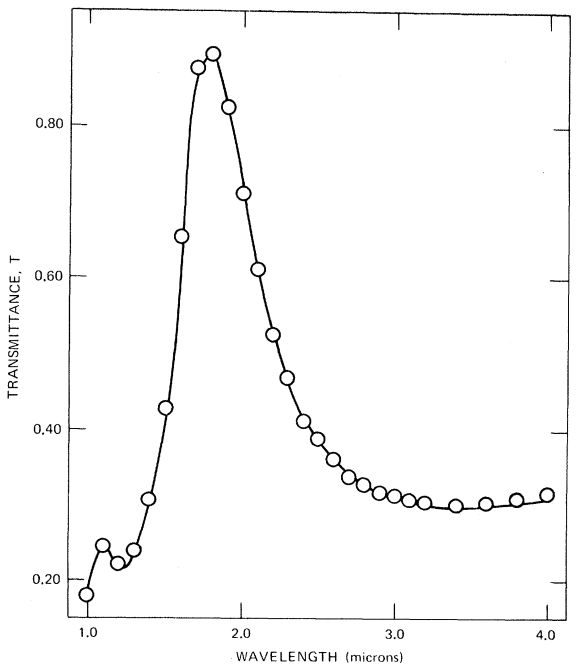

FIG. 3. Values of T_f and T_{calc} for the same film as in Fig. 2.

TABLE I. Measured, corrected, and calculated values of film reflectance and transmittance as well as the calculated optical constants of a 2138-Å amorphous germanium film on fuzed quartz.

Wavelength (μ)	T_{obs}	T_f	T_{calc}	R_{obs}	R_f	R_{calc}	n	k
1.0	0.189	0.181	0.181	0.258	0.257	0.283	4.64	0.41
1.1	0.260	0.248	0.247	0.415	0.412	0.412	4.64	0.27
1.2	0.233	0.221	0.221	0.613	0.611	0.609	4.68	0.18
1.3	0.254	0.240	0.240	0.653	0.651	0.662	4.34	0.11
1.4	0.326	0.309	0.310	0.604	0.601	0.603	4.30	0.08
1.5	...	0.428	0.427	0.483	0.477	0.472	4.26	0.07
1.6	0.681	0.653	0.652	0.283	0.268	0.269	4.20	0.04
1.7	0.908	0.875	0.878	0.118	0.092	0.092	4.18	0.013
1.8	0.925	0.893	0.895	0.074	0.048	0.048	4.28	0.025
1.9	0.855	0.824	0.822	0.160	0.138	0.137	4.12	0.023
2.0	0.741	0.711	0.711	0.283	0.267	0.267	4.11	0.015
2.1	0.640	0.612	0.610	0.402	0.389	0.390	4.09	<0.0025
2.2	0.552	0.526	0.522	0.486	0.478	0.478	4.07	0
2.3	0.492	0.468	0.462	0.544	0.537	0.538	4.08	0
2.4	0.443	0.421	0.417	0.588	0.583	0.583	4.09	0
2.5	0.410	0.389	0.384	0.620	0.615	0.615	4.12	0
2.6	0.384	0.364	0.360	0.643	0.639	0.639	4.24	0
2.7	0.354	0.340	0.340	0.660	0.656	0.655	3.93	0.0076
2.8	0.349	0.331	0.329	0.674	0.670	0.670	3.95	0
2.9	0.338	0.321	0.319	0.683	0.680	0.680	3.97	0
3.0	0.334	0.317	0.313	0.690	0.687	0.687	3.96	0
3.1	0.327	0.311	0.307	0.696	0.692	0.692	3.97	0
3.2	0.325	0.309	0.304	0.699	0.696	0.696	3.98	0
3.3	0.322	0.306	0.301	0.701	0.698	0.698	3.98	0
3.4	0.321	0.305	0.301	0.702	0.699	0.699	3.97	0
3.5	0.321	0.305	0.301	0.702	0.699	0.699	3.97	0
3.6	0.324	0.308	0.302	0.701	0.697	0.697	3.97	0
3.7	0.325	0.309	0.304	0.698	0.696	0.696	3.97	0
3.8	0.329	0.313	0.306	0.697	0.694	0.694	3.97	0
3.9	0.331	0.316	0.308	0.695	0.692	0.692	3.97	0
4.0	0.334	0.319	0.310	0.692	0.689	0.690	3.97	0

small to the lower-energy limit of the measurements. The smallest nonzero values of k in the region of the absorption edge (0.6–0.5 eV) are $k \leq 0.0002$ for a 20654-Å-thick film and $k \leq 0.0004$ for a 12409-Å-thick film. The smaller of these two quantities corresponds to a value of the absorption coefficient $\alpha \leq 10$ cm^{-1}. This value of α has been used, along with photoemission results and the nondirect analysis, to estimate the density of states in the forbidden region.[11] The analysis assumed constant matrix elements and gave a value of 3×10^{17} states/cm^3 for the amorphous Ge samples; this value is less than the 10^{18}–10^{19} states/cm^3 derived from transport measurements[25] and considerably less than the 10^{20} states/cm^3 obtained from recent spin-resonance studies.[10]

For energies lower than 0.31 eV the optical constants were obtained from films deposited on KCl substrates. These latter films were rougher than those deposited on fused-quartz substrates since the KCl surfaces had roughnesses of the order of 100 Å rms. Also, the sample and reference substrates were not as well matched. Because of the large wavelength range (2.0–13.0 μ), it took a longer time to complete a set of measurements, so that aging effects might become important. For these reasons, the low-energy results are not considered as accurate as the higher-energy results in the vicinity of the absorption edge.

Table III gives the optical constants for a 5371-Å-thick Ge film deposited on a KCl substrate in the low-energy range 0.31–0.09 eV (4–13.7 μ). (This is the same film for which optical constants at higher energies are listed in Table II.) The average value of n for this film in the 0.3–0.1-eV region is 3.99 ± 0.04 (the average of 133 data points). This value of n seems to be reasonable since higher-energy n values for this same film (Table II) agree well with n values measured for other Ge films deposited on fused-quartz substrates; it is also within experimental error of the value determined for crystalline Ge in this wavelength range.[26] Furthermore, the reflectance of the 5371-Å-thick Ge film deposited on a fused-quartz substrate in the same evaporation as the sample on the KCl substrate agreed within ± 0.01 of the average re-

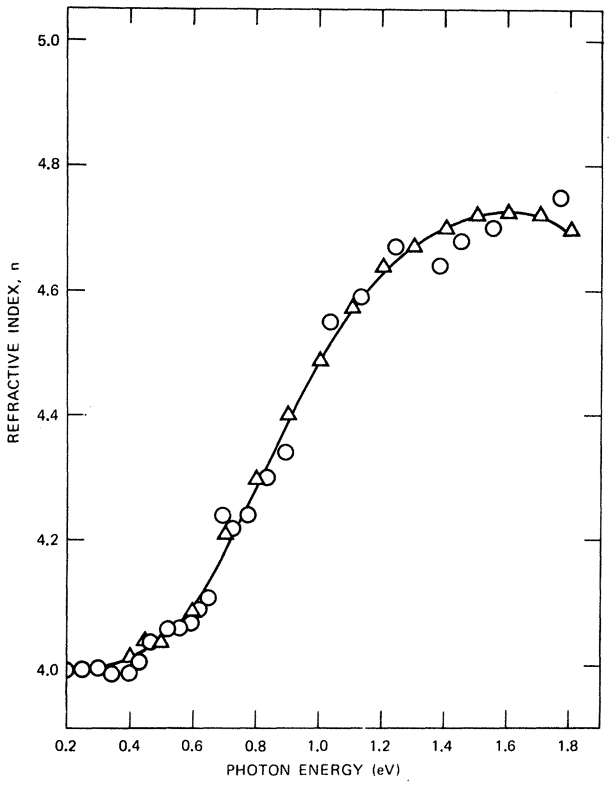

FIG. 4. Measured values of the real part n of the refractive index of amorphous Ge in the region of the absorption edge. The circles are average values for five films obtained from the RT analysis and the triangles are KK analysis results (see Table II). A smooth curve has been drawn through the data points and approaches 4.0 in the low-energy limit.

flectance of films measured in the visible region up to a photon energy of 5.0 eV.

Some variation in low-energy refractive indices has been reported in the literature (see, for example, Ref. 27). We have also observed some variation of n values in this study. One film, deposited using an electron beam gun, had a refractive index of 4.3 at 0.3 eV, considerably higher than the 3.99 average value for the 5371-Å-thick film. Some other films showed a scatter in n values or a reflectance in the visible region well below the average value; these films were not used in the analysis. It is felt that the data presented here are representative of the best obtainable from smooth uniform amorphous Ge films using the reflectance and transmittance (RT) method of analysis.

As can be seen in Table III, the absorption in the low-energy range is quite small, as was also the absorption closer to the edge, which we discussed previously. With the exception of one nonzero value at 0.28 eV, which we feel is an anomalous effect and will be commented on below, there is no evidence for the structure reported by Tauc *et al.*[2] Figure 6 compares our data with that of Tauc *et al.*, where $\epsilon_2 = 2nk$ is plotted versus photon energy. The peaks at 0.16 and 0.30 eV observed in Tauc's data have been interpreted as evidence for direct transitions between heavy and light hole bands in amorphous Ge; the shoulder at 0.8 eV was interpreted as evidence of an appreciable acceptor state density. Tauc *et al.*[2] did not observe this absorption in a more recent study of evaporated films 10–15 μ thick.[9a] In the region centered at about 0.30 eV where Tauc *et al.*[2] reports a large nonzero value of ϵ_2, we obtain a value of zero.

Concerning the k value of 0.012 at 0.28 eV in our data, we feel that it is not an intrinsic property of the Ge since it occurred only at a maximum of transmission, where a small amount of scattering in the film or substrate could reduce the trans-

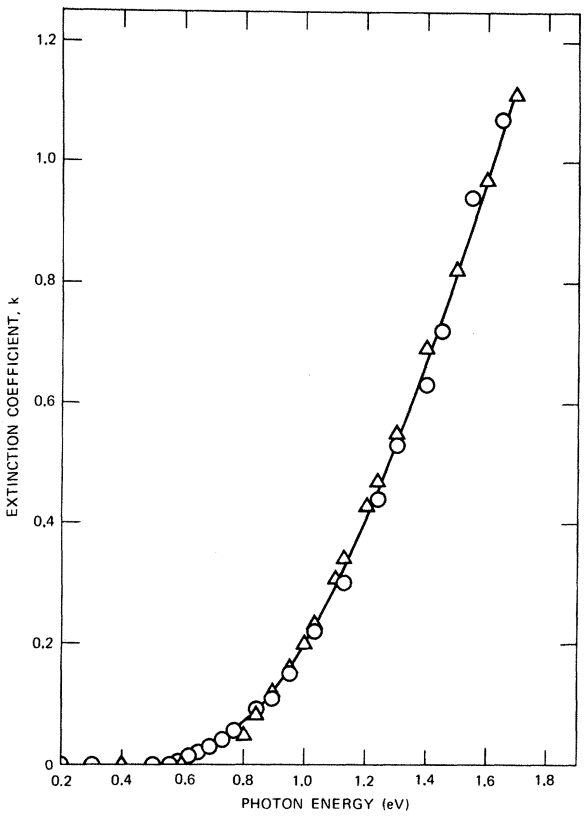

FIG. 5. Measured values for the extinction coefficient k for amorphous Ge in the region of the absorption edge. The circles and triangles have the same meaning as in Fig. 4, and a smooth curve has been drawn through the data points. k approaches zero ($k < 0.001$) at energies lower than 0.58 eV and remains small to the lower-energy limit of the measurements.

TABLE II. The optical constants of five amorphous germanium films from RT analysis. compared with the results of KK analysis

Phonon energy (eV)	Wavelength (μ)	n_a[a]	k_a	n_b	k_b	n_c	k_c	n_d	k_d	n_e	k_e	n_{av}	k_{av}	n_{KK}	k_{KK}
1.24	1.0	4.78	0.46	4.64	0.41	4.58	0.44	...	0.43	...	0.44	4.67	0.44	4.65	0.47
1.13	1.1	4.44	0.35	4.65	0.27	4.59	0.30	4.78	0.28	4.47	0.30	4.59	0.30	4.59	0.34
1.03	1.2	4.77	0.27	4.68	0.18	5.02[b]	0.27	4.31	0.19	4.44	0.20	4.55	0.22	4.51	0.23
0.95	1.3	4.55	0.22	4.35	0.11	4.34	0.15	4.20	0.12	4.12	0.14	4.31	0.15	4.45	0.16
0.89	1.4	4.42	0.17	4.30	0.08	4.32	0.11	4.90[b]	0.09	4.30	0.10	4.34	0.11	4.40	0.12
0.83	1.5	4.34	0.14	4.26	0.07	4.13[b]	0.09	4.08[b]	0.06	4.08[b]	0.08	4.30	0.09	4.33	0.08
0.77	1.6	4.27	0.11	4.20	0.04	4.24	0.05	4.23	0.05	4.69[b]	0.04	4.24	0.06	4.25	0.05
0.73	1.7	4.22	0.08	4.18	0.01[b]	4.29	0.02	3.87[b]	0.02	4.24	0.04	4.22	0.04	4.22	0.03
0.69	1.8	4.18	0.06	4.28	0.03	4.26	0.005	4.40	0.01	4.07	0.03	4.24	0.03	4.20	0.02
0.65	1.9	4.14	0.04	4.12	0.02	3.93[b]	0.005	4.11	0.01	4.08	0.03	4.11	0.02	4.13	0.01
0.62	2.0	4.11	0.02	4.12	0.02	4.02	0.005	4.10	<0.001	4.10	0.02	4.09	0.016	4.10	...
0.59	2.1	4.07	0.0045	4.09	<0.0025	4.03	<0.002	...	...	4.10	0.02	4.07	0.0045	4.09	0.01
0.56	2.2	4.07	<0.0045	4.07	0	4.04	0	4.00	0	4.16	0.02	4.06	<0.001	4.07	<0.001
0.54	2.3	4.07	0	4.08	0	4.04	0	...	...	4.06	0.013	4.06	0	...	0
0.52	2.4	4.06	0	4.09	0	4.04	0	4.04	0	4.07	0.005	4.06	0	...	0
0.50	2.5	4.06	0	4.12	0	4.04	0	...	...	4.08	<0.001	4.07	0	4.05	0
0.48	2.6			4.24[b]	0	4.04	0	4.00	0	4.13	0	4.05	0	...	0
0.46	2.7			3.94	0	4.02	0	...	...	4.17	0	4.04	0	...	0
0.44	2.8			3.95	0	3.84[b]	0	4.11	0	3.89[b]	0	3.97	0	...	0
0.43	2.9			3.97	0	4.05	0	...	...	4.50[b]	0	4.01	0	...	0
0.41	3.0			3.96	0	4.04	0	4.04	0	3.97	0	4.00	0	...	0
0.40	3.1			3.97	0	4.01	0	...	...	3.99	0	3.99	0	4.02	0.0007
0.39	3.2			3.98	0	4.01	0	4.03	0	3.99	0	4.00	0	...	0
0.38	3.3			3.98	0	4.00	0	...	...	4.00	0	3.99	0	...	0
0.36	3.4			3.97	0	4.00	0	4.02	0	4.01	0	4.00	0	...	0
0.35	3.5			3.97	0	3.99	0	...	...	4.00	0	3.99	0	...	0
0.34	3.6			3.97	0	3.99	0	4.02	0	4.01	0	4.00	0	...	0
0.335	3.7			3.97	0	4.00	0	...	...	4.01	0	3.99	0	...	0
0.326	3.8			3.97	0	4.01	0	4.02	0	4.01	0	4.00	0	...	0
0.318	3.9			3.97	0	4.01	0	...	...	4.01	0	3.995	0	...	0
0.310	4.0			3.97	0	4.00	0	4.01	0	4.01	0	4.00	0	4.00	0

[a]Optical constants are for films of the following thickness: (a) 816±4 Å, (b) 2138±10 Å, (c) 3576±13 Å, (d) 5371±4 Å (quartz substrate), (e) 5371±4 Å (KCl substrate).

[b]These points were not used in averaging. They are in error because of measuring errors in R and T resulting from the large oscillations in these quantities.

mittance and appear as anomalous absorption. Further evidence for the correctness of this supposition is that a 9645-Å-thick Ge film deposited on KCl showed no absorption in this energy region, but did show anomalous absorption at other energies where transmission maxima occurred.

Figure 7 compares our values for the absorption coefficient $\alpha = 4\pi k/\lambda$ in the region of the absorption edge (obtained from the smooth curve in Fig. 5) with those of Clark for amorphous Ge[8] and Dash and Newman for crystalline Ge.[28] Note that our absorption edge at about 0.58 eV is comparable in sharpness to the Dash-Newman result for crystalline Ge. Hobden,[29] in a careful study of the absorption edge in crystalline Ge, observed an abrupt change in slope at an energy 0.3 eV above the direct edge. This he interpreted as evidence for the spin-orbit split valence band in crystalline Ge. No evidence is seen for an abrupt change in slope at energies above the absorption edge in either our results or in the Dash-Newman results. As far as magnitude of the absorption is concerned, our present result is in closer agreement with Clark's results[8] in the energy range 0.6–1.1 eV than our previously published data for an 816-Å-thick film (see Ref. 11 and Table II). However, our present result does not show the exponential form in the 0.6–1.24-eV range, which was shown by Clark's data. Although the 816-Å film gave the highest absorption values of any film in this region, there does not seem to be any direct correlation between film thickness and magnitude of absorption.

The position of the absorption edge has been found to be somewhat sensitive to evaporation conditions. Effects of this kind have been reported earlier in studies of amorphous Ge.[27] In the present study, the absorption edge has been found to occur at energies as low as 0.4 eV for films de-

TABLE III. Optical constants[a] in the infrared spectral region for the 5371-Å amorphous germanium film deposited on KCl listed in Table II. The values of the reflectance calculated for a thick sample with no interference effects are also listed.

Photon energy (eV)	Wavelength (μ)	n	k	R
0.310	4.0	4.02	0	0.362
0.282	4.4	4.06	0.012[b]	0.366
0.258	4.8	4.01	0	0.361
0.238	5.2	4.01	0	0.361
0.221	5.6	4.01	0	0.361
0.207	6.0	4.01	0	0.361
0.194	6.4	3.98	0	0.358
0.182	6.8	4.11	0	0.371
0.172	7.2	3.99	0	0.359
0.163	7.6	4.04	0	0.364
0.155	8.0	3.98	0	0.358
0.146	8.5	3.98	0	0.358
0.138	9.0	3.99	0	0.359
0.130	9.5	3.97	0	0.357
0.124	10.0	3.98	...	0.358
0.113	11.0	3.95	0	0.355
0.103	12.0	3.98	0	0.358
0.095	13.0	3.98	0	0.358
0.092	13.5	3.99	0.010	0.359
0.090	13.7	4.01	0.012	0.361

[a]The average of 133 data points in this region gave a value of $n = 3.99 \pm 0.04$ corresponding to a value of $R = 0.359 \pm 0.004$ for the reflectance of a thick sample showing no interference effects.

[b]This value not used (see text).

posited on KCl substrates and for one film deposited on a fused-quartz substrate using an electron beam gun as source. The absorption coefficient α is plotted in Fig. 8 for a 5371-Å-thick Ge film on KCl (triangles) (n and k for this film were used for energies as low as 0.62 eV in the average values in Table II) and a 5445-Å electron beam gun evaporated film on fused-quartz (squares), and compared with the composite results from the five films, shown previously in Fig. 7. The shifted position of the edge could result because there was a greater amount of strain in the two films, or possibly because these films were more highly disordered or less dense than those described above.

Studies of the optical constants of Ge in the region of the absorption edge as a function of disorder through the amorphous-crystalline transition temperature are now in progress and will be described in a later paper.

V. OPTICAL CONSTANTS IN INFRARED, VISIBLE, AND ULTRAVIOLET, DETERMINED FROM A KK ANALYSIS

Optical constants can also be determined from the KK relations between the amplitude and phase of the reflectance, derived by analogy with the well-known dielectric constant dispersion relations. For example, if the reflectance R is known for all frequencies ω between zero and infinity, the phase of the reflectance can also be obtained for all frequencies using the standard integral[30]

$$\theta(\omega) = -(2\omega/\pi)\int_0^\infty \ln[r(\omega')/r(\omega)][1/(\omega'^2-\omega^2)]\,d\omega' \,, \tag{3}$$

where $\hat{r} = re^{i\theta}$ and $R = |\hat{r}|^2$. After the amplitude of the reflectance, r, and the phase θ are obtained, the refractive index n and extinction coefficient k can be determined for all frequencies from the relations

$$n(\omega) = [1 - r^2(\omega)]/[1 + r^2(\omega) - 2r(\omega)\cos\theta(\omega)] \,, \tag{4}$$

$$k(\omega) = 2r(\omega)\sin\theta(\omega)/[1 + r^2(\omega) - 2r(\omega)\cos\theta(\omega)]. \tag{5}$$

Other optical properties can be derived from these expressions, such as the real and imaginary parts of the dielectric constant $\epsilon_1 = n^2 - k^2$ and $\epsilon_2 = 2nk$ and the energy-loss function $-\mathrm{Im}\,(1/\hat{\epsilon})$ (where $\hat{\epsilon}$

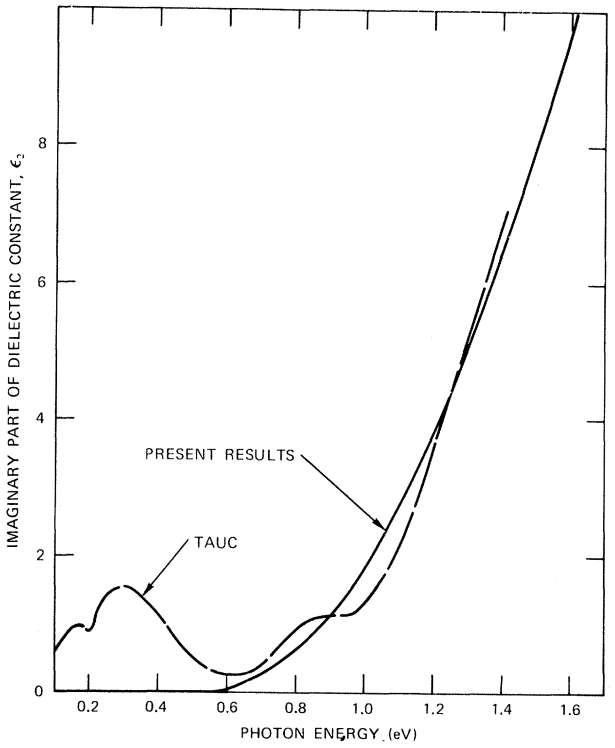

FIG. 6. Comparison of our measured values of $\epsilon_2 = 2nk$ (solid curve) with those reported Tauc *et al.*[2] (dashed curve). The solid curve was calculated from the smooth curves in Figs. 4 and 5. Tauc's reported structure is not seen by him in his later results for thick evaporated films (Ref. 9a).

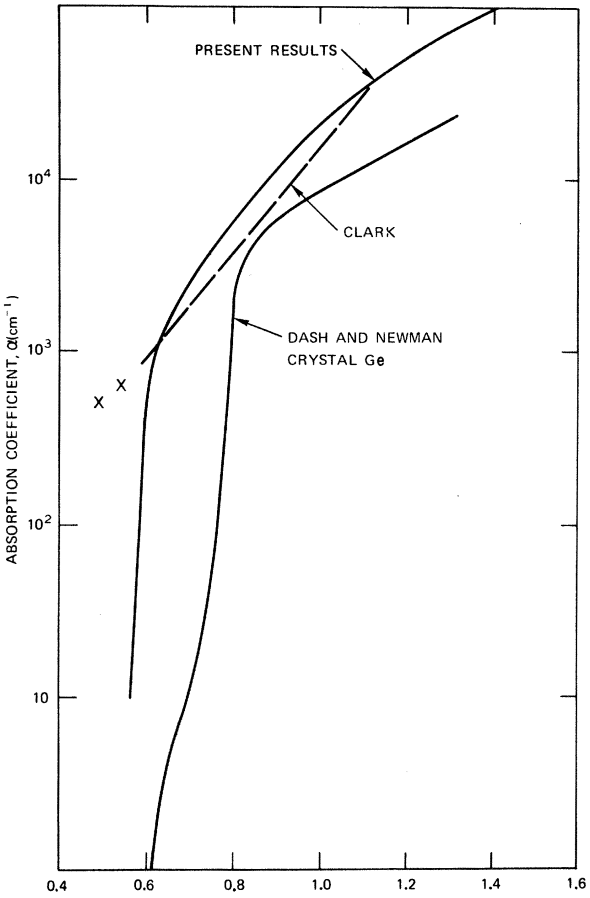

FIG. 7. Comparison of values for the absorption coefficient $\alpha = 4\pi k/\lambda$ of amorphous Ge determined from the smooth k values in Fig. 5 with results of Clark (Ref. 8) and with crystalline results of Dash and Newman (Ref. 28). The absorption edge in amorphous Ge is nearly as sharp as the direct edge in crystalline Ge. The crosses represent data points of Clark which were not included in his exponential plot.

$= \epsilon_1 + i\epsilon_2$).

Since the reflectance R can be measured for only a finite range of frequencies, a suitable extrapolation procedure must be used to generate values of R outside the measured region. At the low-frequency end, a constant value was used for R from the lowest-frequency extrapolated data point at 0.001 eV to $\omega = 0$. The constant extrapolation is justified since the relatively weak lattice bands in crystalline Ge are well separated from the strong absorption at higher energy and, when obtaining optical constants in the high-energy region, the contribution of the lattice bands can be neglected. The reflectances at the last two data points at 0.001 and 0.2 eV used in the KK analysis were adjusted until the phase of the reflectance approached zero smoothly in the infrared. The values for R thus obtained were 0.356 and 0.357, respectively, both within the experimental error of the reflectance of a thick Ge sample calculated from the average value of n in Table III.

At the high-frequency end beyond 25.0 eV, the data were extrapolated using the power law $R = R_0 (E/E_0)^{-A}$, where R_0 is the reflectance at energy E_0 of the last datum point. The constant A was chosen so that the phase angle was equal to the value at 1.4 eV calculated from optical constants obtained from reflectance and transmittance measurements. This value of A was 4.6, close to the value of 4 predicted by the Drude relation (for a free-electron metal) at photon energies much greater than the plasma energy. When the above extrapolation procedure was followed, the phase

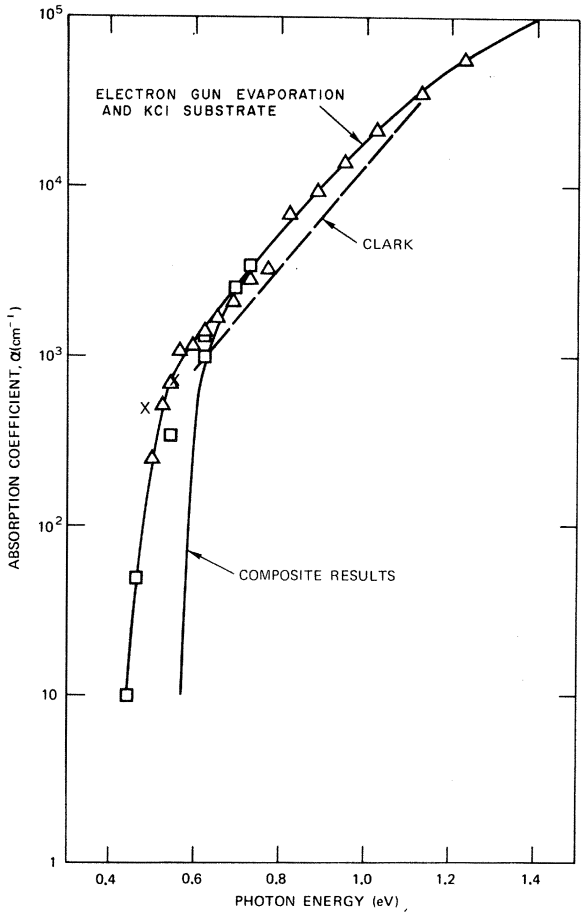

FIG. 8. Variation of α with evaporation conditions. Our composite result and Clark's result from Fig. 7 are compared with values measured for a film evaporated on fused quartz with an electron beam gun (squares) and a film on a KCl substrate (triangles). The curve drawn through these points is shifted about 0.2 eV to lower energy from the results in Fig. 7.

went smoothly to zero at 0.1 eV and k was very small at energies lower than 0.6 eV, in agreement with the experimental results.

Figure 9 shows the composite reflectance curve in the 0.1–25.0-eV region used for the KK analysis. The reflectance[31] of crystalline Ge is also shown as the solid line and Marton and Toots (MT) results[13] (calculated from their n and k data) as the short-dashed line. In the range 0.1–1.2 eV, the reflectance was calculated from smoothed values of n and k from film a in Table II and the film in Table III using the relation

$$R=[(n-1)^2+k^2]/[(n+1)^2+k^2] \ . \qquad (6)$$

This expression assumes a semi-infinite slab of Ge where there are no interference effects within the material or reflection from the back surface. The calculated values agreed within ± 0.01 with the measured normal-incidence reflectance of thick samples in the 1.2–1.8-eV region above the absorption edge.

In the energy range 1.2–5.0 eV, the circles in Fig. 9 represent some of the normal-incidence reflectance measurements made on the Bennett reflectometer using opaque Ge films. These measurements overlap with the *in situ* reflectance measurements made on the Stanford reflectometer, which extend up to 11.8 eV. Between 11.8 and 18 eV, the long-dashed curve is a smooth interpolation

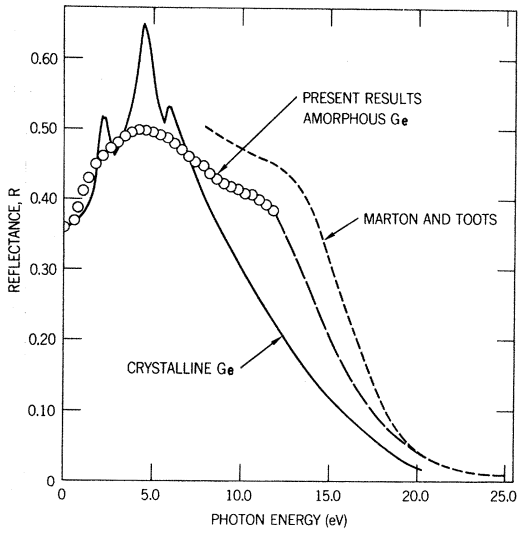

FIG. 9. Reflectance of amorphous Ge in the 0.1–25.0-eV energy range used for the KK analysis. The open circles are measured reflectance values and the long-dashed curve is an interpolation to Marton and Toots's data (Ref. 13) (short-dashed curve) which was used above 20.0 eV. The measured reflectance of crystalline Ge (Ref. 31; solid curve) is also shown for comparison.

to the MT data[13] at 18 eV and above. The shape of the reflectance curve in this region determines the position of the maximum in the volume plasma loss function, and we have drawn the curve so that the maximum occurs at the photon energy found experimentally by MT. At the highest energies, between 20.0 and 25.0 eV, we have used the MT data; because of the small reflectance in this region, the effect of any error in their data would be slight.

In the region of overlap (8.0–11.8 eV), the reason for the difference between our measurements and those of MT is not clear. The difference of 0.05 between the two sets of measurements is outside the range of experimental error of both measurements and could possibly result from actual differences between the two sets of films. It is not caused by contamination or surface plasmon effects, as will be discussed below. Although the MT films were not studied to determine their structural character, they were prepared in a way that would seem to yield amorphous films, judging by the experience gained in the present work. The KK analysis gave similar optical constants in the infrared and absorption-edge regions using either set of data,[11] so it is not possible to distinguish between the two sets of data in this manner. Madden[32] has suggested that differences in the ultraviolet reflectance of evaporated Ge films could be caused by different evaporation rates. He used an evaporation rate of ~500 Å/sec and obtained an initial reflectance value 0.10 higher than our result at 10.2 eV. The MT films were evaporated between 230 and 320 Å/sec, while our films were deposited at less than 50 Å/sec.

The presence of an oxide layer does affect the ultraviolet reflectance of amorphous Ge. By measuring the reflectance in ultrahigh vacuum (*in situ*), breaking vacuum, letting the system up to atmospheric pressure for 1 h, pumping down the system, and remeasuring the reflectance, it was possible to determine the reflectance decrease caused by the oxide layer. Values of this decrease were 0.007 at 3.0 eV, 0.024 at 4.2 eV, and 0.050 at 10.2 eV. The magnitude of the decrease at 10.2 eV agreed with the value reported by Madden[32] which had been obtained under similar conditions. Our results for the ultraviolet reflectance of amorphous Ge, shown in Fig. 9, are not subject to contamination effects because the measurements were completed in about 4 h in a vacuum of 10^{-10} Torr, and no reflectance changes were observed even over a 24-h period at this pressure. Also, no contamination effects have been observed in photoemission data taken over even longer periods using identical vacuum conditions.

Although the dip near 9.0 eV in the measured

reflectance might be caused by a surface plasma resonance excited by slight surface roughness,[33] the difference between our data and the MT data cannot be attributed to this cause. The films used in this study were quite smooth, presumably at least as smooth as the MT films, so both reflectance curves should show the same magnitude of reflectance decrease. Also, the reflectance difference is fairly constant over the whole region of overlap, but surface plasmon excitation normally diminishes quite rapidly on either side of the frequency at which maximum absorption occurs.

When the present reflectance measurements are compared with the reflectance of crystalline Ge (solid curve in Fig. 9), it is seen that there is a broad maximum at 4.4 eV, the same photon energy as that where the reflectance maximum occurs in crystalline Ge, although the fine structure is missing. If the crystalline results were corrected for the effect of an oxide layer, the two curves would be more similar at higher energies. The slight dip in the reflectance of amorphous Ge near 9.0 eV could be caused by surface plasmon excitation since it occurs at an energy slightly lower than that of the maximum in the loss function,[13] consistent with similar effects observed in other materials.[34] Since the crystalline reflectance is dropping so rapidly in this region (even after correction for the effect of an oxide layer), any small change in reflectance caused by surface plasmon absorption would not be observable.

The dip in the reflectance of amorphous Ge manifests itself as a broad peak in the absorption coefficient curve and as a broad shoulder in the optical transition strength curve, both of which will be discussed later. If it is not related to surface plasmon excitation, it could be a density-of-states effect. No structure is observed in the photoemission data at this energy for either clean or cesiated surfaces, which suggests that, if this is a density-of-states effect, transitions are taking place in the region of the vacuum level for the cesiated films (i.e., 2–3 eV or below), which places the initial state density at about 6–7 eV below the maximum level of the filled states. This is the approximate energy where Herman and Van Dyke[4] and Brust[12] place a second maximum in the filled density of states.

The optical constants derived from a KK analysis of the reflectance data in Fig. 9 are shown in Figs. 10 and 11 for the high-energy region, and in Figs. 4 and 5 for the region of the absorption edge. The agreement with values obtained from the RT analysis in the absorption-edge region is excellent. The maximum value of 2.8 in k occurs at 3.8 eV, which is 0.7 eV lower than the highest maximum in crystalline Ge. The n and k curves

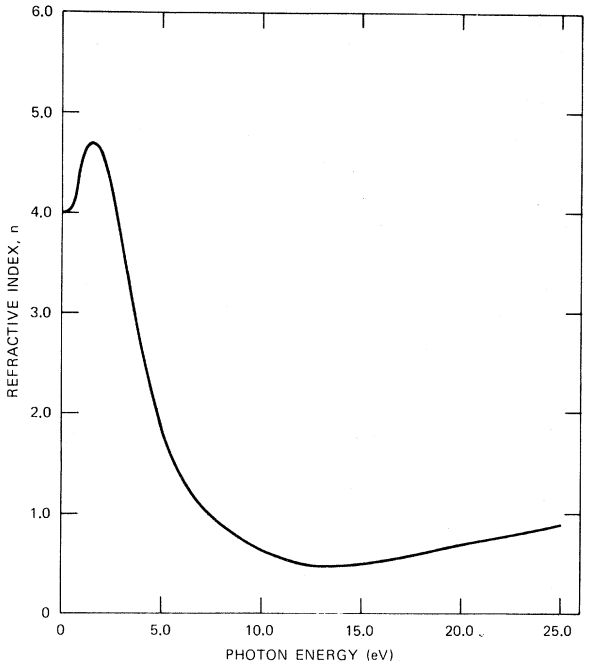

FIG. 10. Real part n of the refractive index of amorphous Ge obtained from the KK analysis.

in Figs. 10 and 11 do not show the detailed structure associated with regions of the Brillouin zone, which is seen in the crystalline optical constants, and are in reasonable agreement with the earlier results of Tauc and Abraham.[34a] There is, however, a rather broad shoulder in k at energies greater than 8.0 eV. This structure is more pronounced in a plot of the optical transition strength, which will be discussed later.

Figures 12 and 13 show values of the dielectric constants ϵ_1 and ϵ_2 derived from n and k. The maximum value of ϵ_2 occurs at 2.8 eV, 1.5 eV lower than the highest maximum in crystalline Ge. The position of the maximum in ϵ_2 has been discussed previously (along with the photoemission results) in terms of the nondirect analysis.[3] Brust[12a] has also discussed the position of the maximum in ϵ_2 and its change with disordering, also taking into account the effect of scattering on direct transitions.

Figures 14 and 15 show the absorption coefficient α and optical transition strength $\omega^2\epsilon_2$, respectively, for amorphous Ge. The broad dip in reflectance centered near 9.0 eV causes a broad peak in α and a broad shoulder in $\omega^2\epsilon_2$. This latter function peaks at 4.3 eV, near where the highest peak occurs in crystalline Ge.

The volume energy-loss spectrum is shown in Fig. 16. The position of the maximum is sensitive to the shape of the reflectance curve above 12.0 eV,

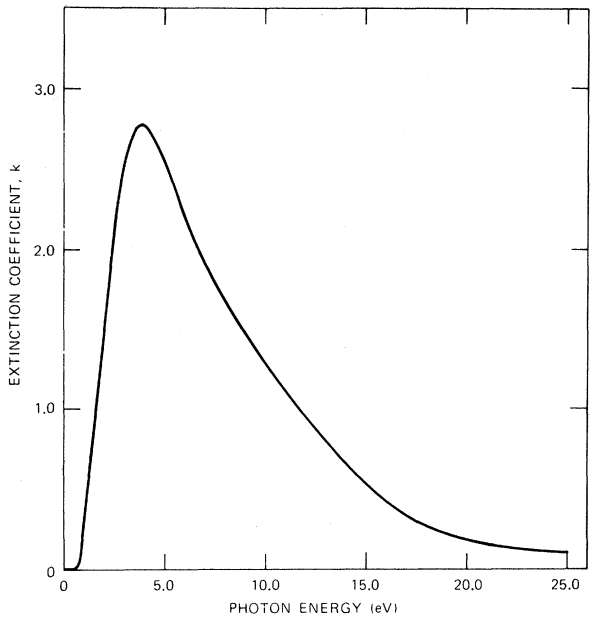

FIG. 11. Extinction coefficient k of amorphous Ge obtained from the KK analysis.

where we have interpolated between our data and that of Marton and Toots, and has varied from 15.6 eV for a reflectance curve steeper than that of MT to 16.6 eV for a shallower interpolation than the one we used. MT found that this function peaked at 16.1 eV, so we have adjusted our interpolation to match this result. Recent fast-electron experiments place the maximum of the energy-loss function at 16.1 ± 0.5 eV.[35] Our maximum value of 2.1 for the loss function is somewhat lower than the value of 3.5 determined by MT and our 5-eV width at half-maximum is somewhat broader than theirs.

VI. SUM-RULE CALCULATIONS

The total optical absorption strength for a material is related to the total number of electrons available to participate in the transitions as determined by the optical sum rules, relations similar to the KK dispersion relations from which they are derived.[30] The sum rule for the optical conductivity is

$$\int_0^E \omega \epsilon_2 \, d\omega = 2\pi n e^2/m \ , \qquad (7)$$

where m is the free-electron mass, e the electronic charge, and n the total electron concentration, equal to the atomic density times the number of participating electrons per atom, $n_{eff}(E)$. If the integral is truncated at some finite energy E, $n_{eff}(E)$ is usually interpreted as the effective number of free electrons contributing to the optical constants in an energy range up to E. Values of $n_{eff}(E)$ are plotted in Fig. 17 and are seen to reach 4.4 electrons/atom if a free-electron mass is used in the calculation. In the preliminary KK analysis published earlier,[11] the exponent in the high-energy power law extrapolation was adjusted so that the reflectance phase was minimized in the infrared. This procedure introduced a single oscillation in the phase in the infrared which gave somewhat different optical constants than would have been obtained if the oscillation had not been present. Since the oscillation was eliminated in this analysis and different ultraviolet reflectances were used, a different $n_{eff}(E)$ was obtained from that reported earlier. Using the new KK results (Fig. 17), n_{eff} goes through 3.9 at 16.1 eV (the volume plasma loss frequency) and rises to 4.4 at 25.0 eV, when the atomic density of crystalline Ge is used. If a slightly lower value were used for the atomic density, n_{eff} would equal 4.0 at the plasma frequency. Since ϵ_2 at the higher photon energies varies with the particular extrapolation procedure used and these values of ϵ_2 contribute significantly to the integral of Eq. (7), the density as determined by direct measurement (see below) is thought to be the more reliable determination.

Feuerbacher *et al.*[36] calculated n_{eff} for crystalline Ge using the MT results between 7.5 and 25.0

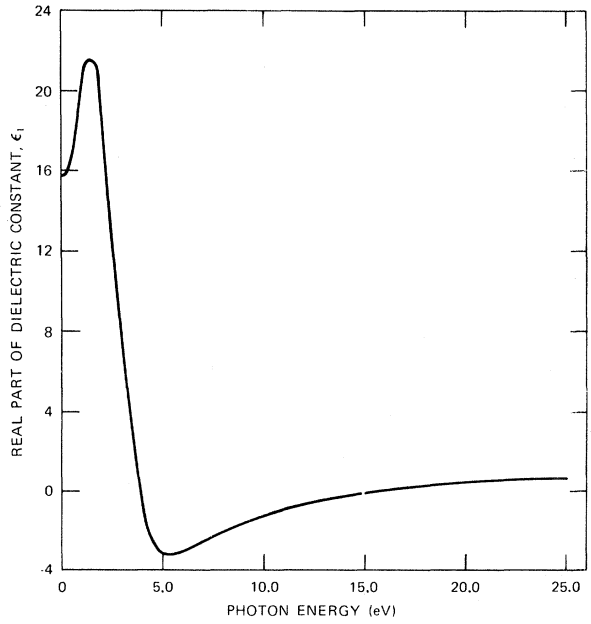

FIG. 12. Real part ϵ_1 of the dielectric constant of amorphous Ge calculated from n and k values in Figs. 10 and 11.

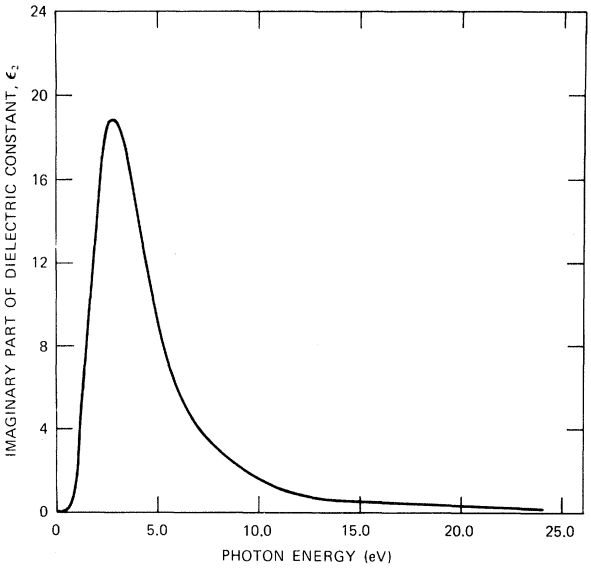

FIG. 13. Imaginary part ϵ_2 of the dielectric constant of amorphous Ge calculated from n and k values in Figs. 10 and 11.

eV (which, as pointed out above, are probably for amorphous films) and their own measurements between 22.5 and 40.0 eV. They found n_{eff} approaching 4.0 at 20.0 eV with the onset of d-band transitions occurring at 35.0 eV.

The plasma frequency was calculated from the relation

$$(\omega_p)^2 = 4\pi ne^2/m \ , \tag{8}$$

using an electron density of 4 electrons/atom and an atomic density equal to that of crystalline Ge. The calculated value was 15.6 eV, which is to be compared with the 16.1-eV value determined by MT from the optical electron loss function and the 15.6–16.6-eV values obtained in the present work. Recent fast-electron experiments,[35] as mentioned above, place the plasma energy loss at 16.1 ± 0.5 eV.

Finally, the effective dielectric constant $\epsilon_{\text{eff}}(E)$ was calculated using the sum rule

$$\epsilon_{\text{eff}}(E) = 1 + \int_0^E (\epsilon_2/\omega)\, d\omega \ . \tag{9}$$

Figure 18 is a plot of $\epsilon_{\text{eff}}(E)$ and is seen to saturate at 15.97 when $E = 20$ eV. This value of the zero-frequency dielectric constant yields a zero-frequency refractive index of 4.00, in excellent agreement with the value of 3.99 (in the infrared) determined from the RT measurements.

VII. DENSITY DETERMINATION

We measured the density of amorphous Ge on films prepared under the same conditions as the optical samples by weighing thin aluminum foils before and after depositing relatively thick (1-μ) Ge films. The thicknesses of the films were determined interferometrically (see Sec. II) and the lateral dimensions were measured using an optical comparator. The density of amorphous Ge determined in this manner was 4.54 ± 0.14 g/cm^3, about 15% less than that of crystal-line Ge. This result was for films deposited under standard vacuum conditions. For thinner films (~2500 Å) deposited in ultrahigh vacuum, the result was somewhat higher, 4.73 ± 0.05 g/cm^3. The precision of a given measurement was of the order of 1–4%, depending on thickness. Similar measurements on 2000-Å polycrystalline films gave densities within 3% of bulk. Our measured density is closer to the crystalline value than Clark's value of 3.9 ± 0.4 g/cm^3 obtained by weighing thicker films that had shattered and separated from the substrates.[8] We have recently obtained values of 4.1–4.2 g/cm^3 lower than the 4.54 g/cm^3 reported above by evaporating Ge films using a smaller source-to-substrate distance (13 in.), but the same evaporation rate as that used for the rest of the measurements described in this paper.

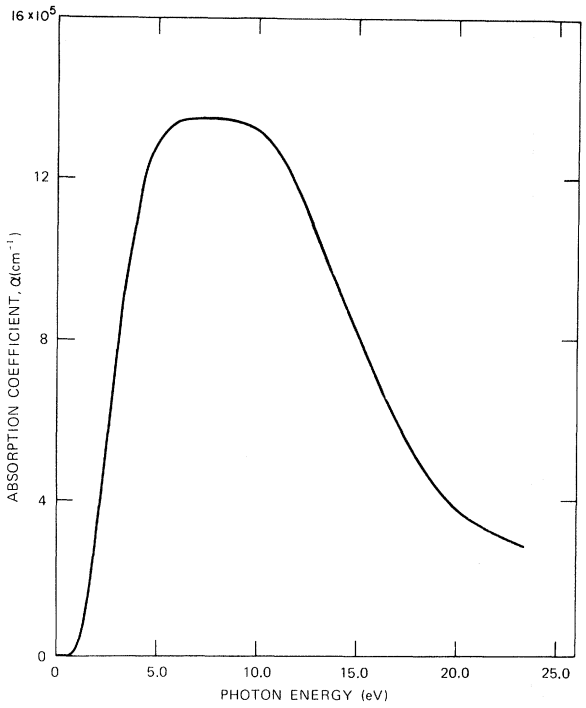

FIG. 14. Absorption coefficient α of amorphous Ge calculated from k values in Fig. 11. The shoulder at 9.0 eV is caused possibly by excitation of a surface plasmon or by a density-of-states effect.

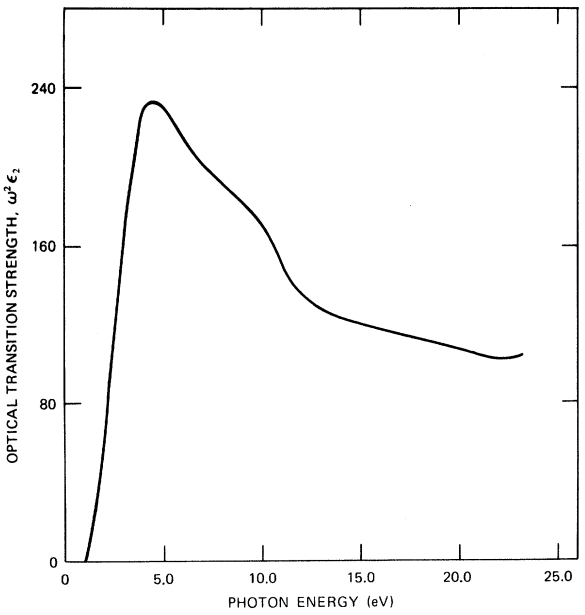

FIG. 15. Optical transition strength $\omega^2\epsilon_2$ for amorphous Ge calculated from values of ϵ_2 in Fig. 13. The shoulder at 9.0 eV in α (Fig. 14) is seen more clearly in this curve.

Whether the source-to-substrate distance, evaporation rate, presence of pin holes or voids, or other factors affect the density of amorphous Ge is not clear. In any case, our value of 4.54–4.78 g/cm^3 is outside the experimental uncertainty of a recent determination[37] in which the density of amorphous Ge was found to be equal to that of crystalline Ge.

VIII. CONCLUSIONS

The following conclusions can be drawn from the optical constants determined from reflectance and transmittance measurements on amorphous Ge: (a) The absorption edge is quite sharp, with a width comparable to that for the direct edge in crystalline Ge. It occurs at an energy of about 0.6 eV, 0.2 eV lower than the direct edge in crystalline Ge. The edge has been observed to move to lower energy (0.4 eV) under some evaporation conditions. There is no indication of absorption which could be associated with a spin-orbit split valence band, as observed by Hobden for crystalline Ge. (b) There is no evidence for a tailing of states into the forbidden gap or for large numbers of states in the gap. The smallest nonzero value of the absorption coefficient measured on the low-energy side of the absorption edge was about 10 cm^{-1}. This value of the absorption coefficient has been used to obtain an estimate of $<10^{18}$ states/cm^3 for the number of states in the forbidden gap, which is in reasonable agreement with the number determined from transport measurements, but considerably less than the number determined from spin-resonance studies. (c) No "free-carrier" absorption was observed in the infrared region out to 13 μ. (d) The average value of the index of refraction between 0.1 and 0.3 eV determined from the *RT* analysis was 3.99 ± 0.04. This is close to the value obtained for crystalline Ge in this wavelength range.

The position and sharpness of the absorption edge, as well as the value of the zero-frequency dielectric constant, have been verified using a KK analysis of the normal-incidence reflectance data. The static dielectric constant ϵ_{eff} determined by a sum-rule calculation on ϵ_2 is 16.0 for amorphous Ge, in good agreement with the dielectric constant at 0.1 eV determined from the *RT* analysis. The average values of n and k in the 0.1–1.24-eV region determined from the KK and *RT* analyses are listed in Tables II and III. The density as determined by direct measurement was found to be 12–15% less than the crystalline density.

ACKNOWLEDGMENTS

We would like to thank J. Dancy and R. L. Peck

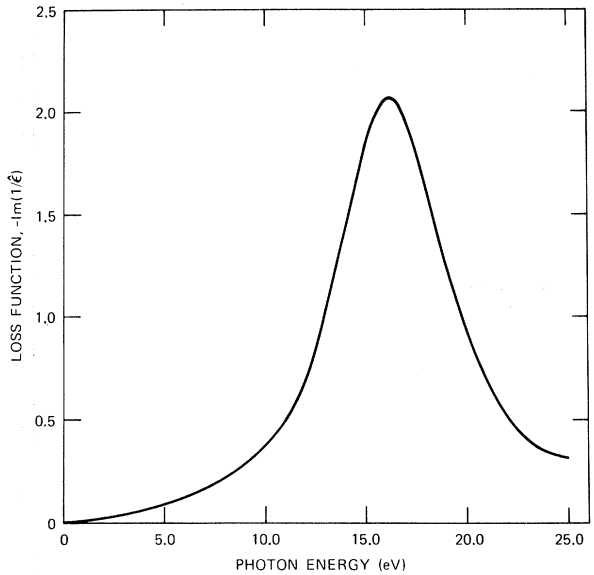

FIG. 16. Electron energy-loss function $-\mathrm{Im}(1/\hat{\epsilon})$ for amorphous Ge calculated from values of ϵ_1 and ϵ_2 in Figs. 12 and 13, respectively. The reflectance curve for the KK analysis in Fig. 9 was interpolated between our measured curve and that of Marton and Toots so that the peak of the loss function would occur at the same energy as in Ref. 13.

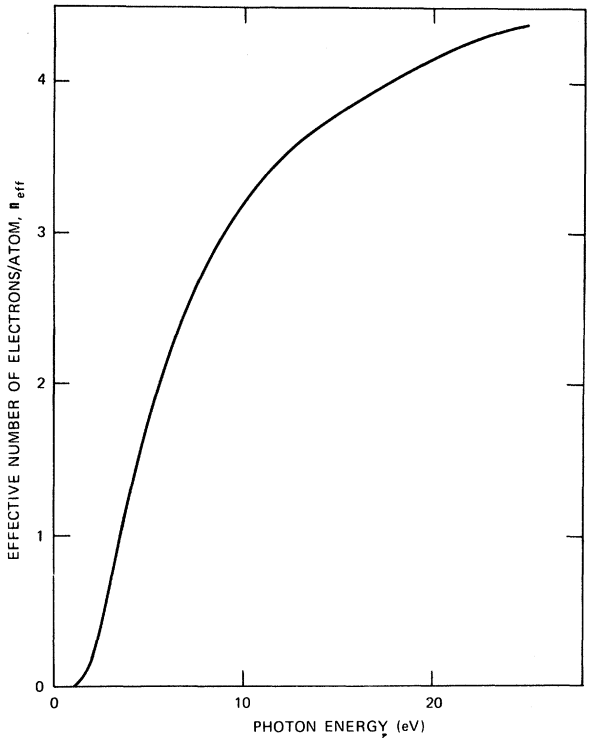

FIG. 17. The effective number of electrons/atom involved in transitions up to an energy of 25.0 eV. The value of 4 electrons/atom is reached at 17.6 eV, about 1.5 eV higher than the peak in the electron energy-loss function.

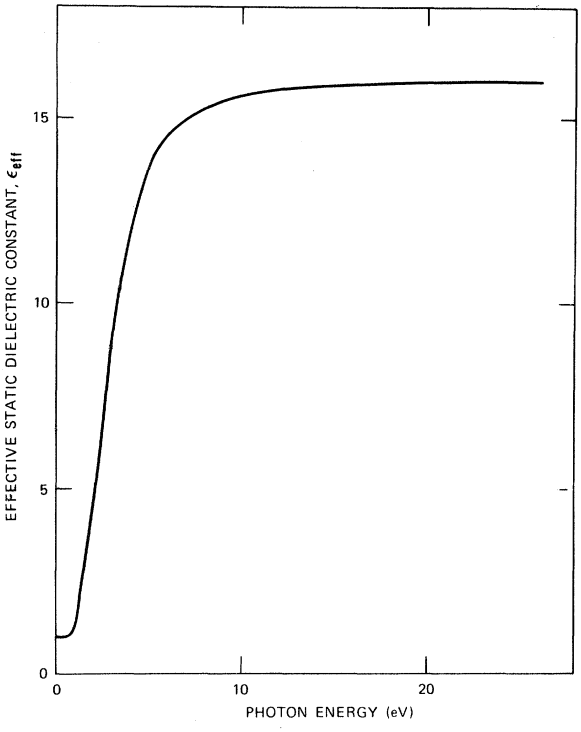

FIG. 18. The effective static dielectric constant ϵ_{eff}. The saturation value of 16.0 for this function is reached at 17 eV and yields a zero-frequency refractive index of 4.0, the same as that determined from the *RT* analysis.

for electron and x-ray diffraction studies of the Ge films, H. E. Bennett for helpful discussions, and D. L. Decker for extensive discussions of the KK analysis and the use of his computer program.

---

*Work supported in part by the Advanced Research Projects Agency through the Center of Materials Research, Stanford University, Stanford, Calif. 94305 and by the Director of Naval Laboratories.

†Permanent address: Michelson Laboratory, China Lake, Calif. 93555.

[1]T. M. Donovan and E. J. Ashley, J. Opt. Soc. Am. 54, 1141 (1964).

[2]J. Tauc, R. Grigorovici, and A. Vancu, Phys. Status Solidi 15, 627 (1966).

[3]T. M. Donovan and W. E. Spicer, Phys. Rev. Letters 21, 1572 (1968).

[4]F. Herman and J. P. Van Dyke, Phys. Rev. Letters 21, 1575 (1968).

[5]A. I. Gubanov, *Quantum Electron Theory of Amorphous Conductors* (Consultants Bureau Enterprises, Inc., New York, 1965).

[6]N. F. Mott, Advan. Phys. 16, 1 (1967).

[7]N. F. Mott, Contemp. Phys. 10, 125 (1969).

[8]A. H. Clark, Phys. Rev. 154, 750 (1967).

[9](a) J. Taue, A. Abraham, R. Zallen, and M. Slade, J. Non-Cryst. Solids 4, 233 (1970); (b) see also J. Wales, G. J. Lovitt, and R. A. Hill, Thin Solid Films 1, 137 (1967).

[10]M. H. Brodsky and R. S. Title, Phys. Rev. Letters 23, 581 (1969).

[11]T. M. Donovan, W. E. Spicer, and J. M. Bennett, Phys. Rev. Letters 22, 1058 (1969); W. E. Spicer and T. M. Donovan, J. Non-Cryst. Solids 2, 66 (1970).

[12](a) D. Brust, Phys. Rev. Letters 23, 1232 (1969); and D. Brust, Phys. Rev. 186, 768 (1969); (b) K. L. Chopra and S. K. Bahl, Phys. Rev. B 1, 2545 (1970).

[13]L. Marton and J. Toots, Phys. Rev. 160, 602 (1967).

[14]R. W. Dietz and J. M. Bennett, Appl. Opt. 5, 881 (1966).

[15]H. E. Bennett and W. F. Koehler, J. Opt. Soc. Am. 50, 1 (1960).

[16]H. E. Bennett, Appl. Opt. 5, 1265 (1966).

[17]H. E. Bennett and J. M. Bennett, in *Physics of Thin Films*, edited by G. Hass and R. E. Thun (Academic, New York, 1967), Vol. 4, pp. 31-37.

[18]E. Krikorian and R. J. Sneed, J. Appl. Phys. 37,

3665 (1966).
[19]J. Endriz, Ph.D. thesis, Stanford University (unpublished).
[20]W. F. Koehler, J. Opt. Soc. Am. 45, 934 (1955).
[21]See Ref. 17, pp. 42–44.
[22]P. H. Berning, in *Physics of Thin Films*, edited by G. Hass (Academic, New York, 1963), Vol. 1, pp. 69–121.
[23]J. M. Bennett and M. J. Booty, Appl. Opt. 5, 41 (1966).
[24]G. Hass, in *American Institute of Physics Handbook*, 2nd ed., edited by D. E. Gray (McGraw-Hill, New York, 1963), pp. 6–105.
[25]R. Grigorovici, N. Croitoru, A. Dévényi, and E. Teleman, in *Proceedings of the Seventh International Conference on the Physics of Semiconductors, Paris, France*, 1964 (Academic, New York, 1964), p. 423.
[26]T. M. Donovan (unpublished); C. D. Salzberg and J. J. Villa, J. Opt. Soc. Am. 47, 244 (1957).
[27]See Ref. 9(b).
[28]W. C. Dash and R. Newman, Phys. Rev. 99, 1151 (1955).
[29]M. V. Hobden, J. Phys. Chem. Solids 23, 821 (1962).
[30]F. Stern, in *Solid State Physics*, edited by F. Seitz and D. Turnbull (Academic, New York, 1963), pp. 299–408.
[31]H. R. Philipp and H. Ehrenreich, Phys. Rev. 129, 1550 (1963); T. M. Donovan, H. E. Bennett, and E. J. Ashley, J. Opt. Soc. Am. 53, 1403 (1963).
[32]R. P. Madden, in *Physics of Thin Films*, edited by G. Hass (Academic, New York, 1963), Vol. 1, pp. 123–186.
[33]S. N. Jasperson and S. E. Schnatterly, Bull. Am. Phys. Soc. 12, 399 (1967).
[34]J. L. Stanford, J. Opt. Soc. Am. 60, 49 (1970).
[34a]J. Tauc and A. Abraham, Czech. J. Phys. 19, 1246 (1969).
[35]See Ref. 13 for a discussion of fast-electron energy loss measurements.
[36]B. Feuerbacher, M. Skibowski, R. P. Godwin, and T. Sasaki, J. Opt. Soc. Am. 58, 1434 (1968).
[37]T. B. Light, Phys. Rev. Letters 22, 999 (1969).

PHYSICAL REVIEW B VOLUME 2, NUMBER 2 15 JULY 1970

Influence of Self-Induced Magnetic Field on the Stability of an Electron-Hole Plasma in Parallel Electric and Magnetic Fields*

B. V. Paranjape and K. C. Ng
Department of Physics, University of Alberta, Edmonton, Alberta, Canada
(Received 10 September 1969; revised manuscript received 26 March 1970)

The Kadomtsev-Nedospasov theory of helical instability of a gaseous plasma has been applied to semiconductors by several authors. We have extended this theory to include the force arising from a self-induced magnetic field. Such a force pulls the plasma to the center. Helical instability is due to the flux of charged particles to or from the surface, and thus depends on the surface conditions. We have treated the effect of the self-induced field as a small perturbation on this surface effect. It is predicted that the stability increases or decreases if the flux due to the self-induced field adds or substracts from the flux due to boundary conditions.

INTRODUCTION

The onset of current oscillations[1–4] in semiconductors placed in parallel electric and magnetic fields is in some cases due to helical instabilities set up in the material. The theory of helical instability was first presented by Kadomtsev and Nedospasov.[5] The original Kadomtsev-Nedospasov paper is on gaseous plasma. Their ideas have been applied to plasma in semiconductors by several authors.[6–8] One solves the problem of